Evaluation of Neurovascular Coupling Behaviors for FES-Induced Wrist Movements Based on Synchronized EEG-fNIRS Signals

He Mao, Haotian Meng, Qiyun Tan, Oluwarotimi Williams Samuel, *Senior Member, IEEE*, Guanglin Li, *Senior Member, IEEE*, and Peng Fang, *Senior Member, IEEE*

***Abstract*— The neuronal activities and cerebral hemodynamic responses are closely linked via the neurovascular coupling (NC) mechanism. This mechanism is strongly associated with the brain state and alters with the pathological conditions such as motor dysfunctions. Clinically, functional electrical stimulation (FES) is being increasingly used for motor function restoration, but the impact of FES on NC behaviors is still lack of study, which would prevent the understanding of FES in improving neurorehabilitation performance. In this work, we studied the NC behaviors based on synchronously recorded electroencephalography and functional near-infrared spectroscopy (EEG-fNIRS) signals during FES-induced wrist movements from twenty healthy subjects. Oxygenated (HbO) and deoxygenated (HbR) hemoglobin concentrations were computed from the fNIRS signals, event-related (de-)synchronization (ERD/ERS) was computed from the EEG in alpha and beta bands, and transfer entropy (TE) was used to assess the coupling between the two signals. Experimental results revealed that the NC behavior of FES-induced movements was similar to that of voluntary movements, with a slower HbO activation process but longer duration. A bidirectional coupling relationship was observed between EEG power envelope and HbO time series but the TE from HbO to EEG ($TE_{HbO\rightarrow EEG}$) was larger than that for the opposite direction. Significant differences were found between the FES-induced and voluntary tasks, where the former showed higher $TE_{HbO\rightarrow EEG}$ on the ipsilateral sensorimotor cortex than the latter, which indicates that FES could improve the regulatory effect of ipsilateral cerebral blood flow on neuronal activities. This work may contribute to understanding the neurorehabilitation mechanism by FES and provide evidence-based support for clinical application from the perspective of NC.**

***Index Terms*— Neurovascular coupling, functional electrical stimulation, EEG, fNIRS, rehabilitation.**

I. Introduction

FUNCTIONAL electrical stimulation (FES) is a common clinical method used to restore the limb motor function in paralyzed patients [1], [2]. Clinical reports have shown that FES can prevent prolonged loss of neuromuscular function and indirectly maintain cardiopulmonary health [3], [4], where the benefits of FES are known to be associated with the Hebbian theory [5] and central pattern generator [6], [7]. However, the study of the underlying neurorehabilitation mechanism of FES remains insufficient, particularly from the perspective of neurovascular coupling (NC) [8], [9], which has recently been linked to many central nervous system diseases.

The concept of NC was first proposed by Roy and Sherrington in the 1890s [10]. It refers to the tight regulatory mechanism between localized neuronal activity and cerebral blood flow (CBF), which rapidly increases to ensure the working neurons can obtain sufficient oxygen and nutrients. NC is generally associated with the health state of the brain, while in pathological conditions such as hypertension, Alzheimer's disease, and ischemic stroke, NC is usually disrupted, preventing CBF from matching the metabolic needs of affected tissues [11], [12]. The research progress on NC mechanisms, along with advancements in modern brain functional imaging techniques, has ushered in a new era in neuroscience research and development.

A simultaneous measurement of electroencephalography and functional near-infrared spectroscopy (EEG-fNIRS) signals has become a powerful tool for probing NC in both normal states and diseases [13], [14]. EEG captures the temporal dynamics of brain electrical activities by measuring voltages generated by macroscopic currents within neuronal ensembles [15]. It has an excellent temporal resolution but a limited spatial resolution [16]. fNIRS monitors the hemodynamic responses and oxygenation changes evoked by neuronal activities [17]. It can measure the concentration changes of oxygenated (HbO), deoxygenated (HbR), and total (HbT) hemoglobin at the capillary level [18]. In contrast to EEG,

Received 7 December 2024; revised 10 April 2025; accepted 1 July 2025. Date of publication 4 July 2025; date of current version 15 July 2025. This work was supported in part by Shenzhen Basic Research Foundation under Grant JCYJ20230807140817037 and Grant JCYJ20241202124935047, in part by the National Natural Science Foundation of China under Grant U21A20479, in part by the Chinese Academy of Sciences (CAS) Youth Innovation Promotion Association under Grant Y2022094, and in part by Shenzhen Engineering Laboratory of Neural Rehabilitation Technology. *(Corresponding author: Peng Fang.)*

This work involved human subjects or animals in its research. Approval of all ethical and experimental procedures and protocols was granted by the Institutional Review Board of Shenzhen Institutes of Advanced Technology, Chinese Academy of Sciences under IRB No. SIAT-IRB-230915-H0670.

He Mao, Haotian Meng, Qiyun Tan, Guanglin Li, and Peng Fang are with Shenzhen Institutes of Advanced Technology, Chinese Academy of Sciences, Shenzhen 518055, China (e-mail: peng.fang@siat.ac.cn).

Oluwarotimi Williams Samuel is with the School of Computing and Data Science Research Centre, University of Derby, DE22 3AW Derby, U.K.

Digital Object Identifier 10.1109/TNSRE.2025.3585883

fNIRS has a relatively better spatial resolution but lower temporal resolution due to the slow hemodynamic response [19], [20]. Therefore, EEG and fNIRS may complement each other for more diverse and complete neurophysiological information associated with NC. EEG and fNIRS are both noninvasive scalp-located signal acquisition technologies, and especially the electro-optical interference is quite tiny that can be ignored. Hence, integrating EEG and fNIRS into a simultaneous multimodal signal acquisition system benefits the evaluation of neurovascular interactions in various tasks.

In recent years, a number of studies have described the NC phenomena between brain rhythmic activities and cerebral hemodynamic responses. During voluntary movements, such as self-paced finger movements [21] and ankle joint movements [22], a noticeable increase in HbO and a decrease in HbR concentration were observed, with the amplitude of alpha and beta EEG rhythms decreased. Besides, negative correlations were found between alpha/beta ERD and HbO, while positive correlations were found between these rhythms and HbR. Regarding FES-induced movements, a previous study found that a motor imagery brain-computer interface combined with FES could induce strong ERD and blood oxygenation responses, but the ipsilateral cerebral hemodynamic response was not investigated [23]. In addition, different evaluation methods were proposed to quantify the NC functional impairment for various diseases. For ischemic stroke, a related study evaluated the NC relationship between EEG band power and HbO signals through an autoregressive model [24]. Another study proposed an NC model based on Hilbert-Huang Transform to evaluate the impaired NC function [25]. For Alzheimer's disease, several global NC features were proposed using a general linear model framework by regressing whole-head EEG power envelopes of different frequency bands with average HbO and HbR changes in the frontal and prefrontal cortices [26], [27]. Nevertheless, previous NC-related studies utilizing EEG-fNIRS multimodal signals mainly focused on NC monitoring and finding appropriate evaluation methods. The effect of FES on neuronal activities and cerebral blood perfusion has rarely been studied, and thus the induced neurovascular interaction alteration needs further exploration.

To address the above issues, this study used an integration of EEG-fNIRS signals to investigate how FES affects brain rhythmic activities and cerebral hemodynamic responses on bilateral sensorimotor cortices (SMCs), with voluntary movements investigated as a control condition. Transfer entropy (TE) was implemented to explore the neurovascular interaction, i.e., the bidirectional coupling relationship, between the electrophysiological and hemodynamic variables. This work aims to provide NC evidence to support FES therapy and a practical TE-based approach in constructing objective biomarkers.

II. Data and Methodology

A. Subjects and Experimental Protocol

Twenty healthy volunteers (all male and right-handed, with ages of 23-38 years old) were recruited. All participants gave their written consent after a detailed explanation of experiment procedure and possible risks associated with the designed

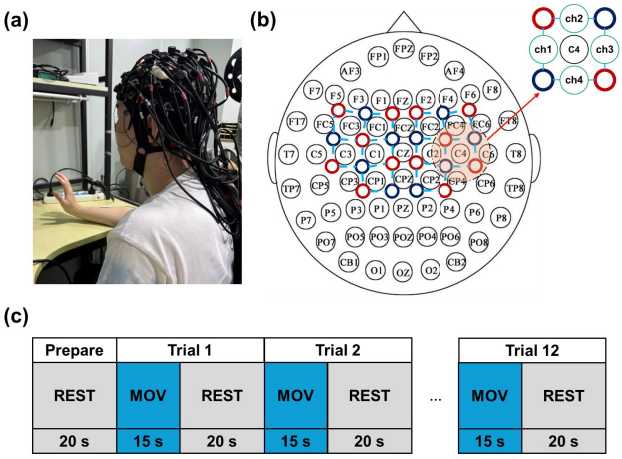

Fig. 1. (a) Experimental set up for simultaneous EEG-fNIRS measurement during wrist extension. (b) Distribution of EEG electrodes (black circles), fNIRS source (red circles) and detector probes (blue circles) on the scalp. The location of a fNIRS channel was defined as the midpoint of a source-detector pair. Four fNIRS channels were evenly distributed around each EEG electrode, as shown in an enlarged view of position C4, where green circles represent fNIRS channels. (c) Time scheme of the experiment protocol.

experiments. The experiment protocol was approved by the Institutional Review Board of Shenzhen Institutes of Advanced Technology, Chinese Academy of Sciences (*IRB Number: SIAT-IRB-230915-H0670*).

In the data collection session, participants sat comfortably in a dark, electrically shielded room with their eyes open. As shown in Fig. 1(a), each participant's head was covered with a specially designed head cap for simultaneous EEG-fNIRS recording. The cap was developed by pouncing small holes on a standard EEG cap (*Wuhan Greentek Pty. Ltd, China*) and mounting special flanges to fix the fNIRS probes. Fig. 1(b) shows the distribution of EEG electrodes, and fNIRS source and detector probes on the scalp.

Each participant was asked to put their right forearm on a desk to perform two predefined wrist movement tasks: (i) voluntary wrist extension (VOL) and (ii) FES-induced wrist extension (FES). In the VOL task, participants were instructed to follow the instructions displayed on a computer screen. They performed maximum wrist extension five times during a 15-s movement period (i.e., extend the right wrist and return to the neutral position in 3 s, totally for five times). In the FES task, an isolated bipolar constant current stimulator (*DS5, Digitimer Ltd., UK*) was used to provide a biphasic electrical stimulation with 300-μs pulse width and 30-Hz frequency. Two electrodes (6×4.5 cm^2) were positioned near the motor points of the wrist extension muscles, at approximately 1/2 and 1/3 of the dorsal forearm. To achieve maximum wrist extension, the stimulation current amplitude was adjusted in a range from 12 to 18 mA for each participant. One block of electrical stimulation lasted for 3 s, with a 1.5-s on and 1.5-s off period. A total of five blocks were presented during each movement period to induce wrist extension five times. Thus, in both tasks, each movement period lasted for 15 s, containing five maximum wrist movements. Besides, a 20-s rest period was provided afterwards to avoid possible experiencing fatigue, which might affect the quality of recordings. The above movement paradigms were designed to induce obvious

cerebral hemodynamic responses and provide sufficient time to recover to the baseline. Twelve trials were recorded for each task and the duration of experiment is shown in Fig. 1(c).

B. EEG Recording and Processing

The EEG data were acquired using the Neuroscan's SynAmps^{2TM} system (*Compumedics Neuroscan USA Ltd., USA*). Ag/AgCl electrodes were placed on the scalp of each participant following the international 10/20 system. Additional six electrodes were placed at the left and right mastoids (M1 and M2), the outer canthi of both eyes (HEOL and HEOR), and the infraorbital and supraorbital regions of the left eye (VEOL and VEOU). Skin/electrode impedance was measured before recording and conductive paste was applied to maintain the impedance below 5 kΩ. EEG data were sampled at 1000 Hz.

The acquired EEG data were stored and preprocessed off-line using the EEGLAB toolbox in MATLAB (*The Mathworks, USA*) [28]. EEG data were re-referenced to both mastoids (M1 and M2) and filtered within the range 1-47 Hz. They were then segmented into epochs (−5 to 30 s) according to markers and baseline corrected (−5 to -2 s). Afterwards, muscle and eye artifacts were isolated and removed from the data using the independent component analysis (ICA) technique. Finally, the EEG waves were visually inspected, and contaminated trials in the data were manually rejected.

Event-related (de-)synchronization (ERD/ERS) is often used to evaluate brain functional activation. It can reflect EEG energy changes in SMC before, during, and after movements [29]. To calculate the ERD/ERS time-frequency maps, the preprocessed EEG data were down-sampled to 128 Hz. Short Time Fourier Transform was applied to each trial, and the spectrogram was baseline-corrected in the time-frequency domain using a reference epoch of (-5 to -2 s).

To compute the ERD/ERS time courses, the preprocessed EEG data were decomposed into two frequency bands of interest, i.e., alpha: 8-13 Hz and beta: 13-30 Hz. The power envelope of each trial was computed as the absolute value of the Hilbert Transform. The ERD/ERS time courses were computed as relative change expressed in percentage according to the formula defined in [30].

$$ERD/ERS = \frac{\left[P(t,f) - \bar{R}(f)\right]}{\bar{R}(f)} \times 100\% \qquad (1)$$

where, $P(t, f)$ denotes spectral power at point(t, f) in the time-frequency map, and $R(f)$ denotes the spectral power in reference epoch and its average is $\bar{R}(f)$.

To form a topographic distribution of ERD, the EEG data were re-referenced to a common average. Then, the ERD/ERS time courses were calculated for all EEG channels, normalized to z-values, and averaged over the movement period (0-15 s).

C. fNIRS Recording and Processing

The fNIRS data were recorded using a multi-channel oxygenation monitor operating at wavelengths of 730 and 850 nm (*NirScan-400, Danyang Huichuang Medical Equipment Co., Ltd., China*). Twelve optical source probes and ten detector probes were used to form a montage of 30 fNIRS channels symmetrically covering the bilateral SMCs. The distance between a source and neighbouring detector probe was 3 cm, and the location of a fNIRS channel was defined as the midpoint of a source-detector pair. After brushing each participant's hair aside and exposing their scalp, optical probes were plugged into mounting holes and fixed on the cap with special buckles to ensure that the channels were properly fitted for high-quality data recording. The fNIRS sampling frequency was set to 17 Hz. The *E-prime* software was used to instruct the participants to move their wrists in a VOL task, or guide the experimenter to perform FES in a FES task. It also sent trigger signals to the EEG and fNIRS acquisition software through a synchronization box to mark the start of each experimental trial.

The aquired fNIRS data was preprocessed off-line using the *NirSpark* software package [31]. Firstly, the raw light intensity signals were converted into optical density (OD) data. Secondly, the motion artifacts in the data were removed. Then, a Butterworth band-pass filter (0.01-0.2 Hz) was used to remove physiological noises caused by heartbeat and respiration. Thereafter, the OD data were converted to relative concentration changes of HbO and HbR based on the modified Lamber-Beer law, with all differential path-length factors (DPF) set to 6 [32], [33].

The detailed motion artifact correction method used in this study was as follows. We detected signals that the amplitude and standard deviation exceeded the thresholds within a predefined time window and marked the data points around the detected motion as artifacts. The standard deviation threshold was set to 6, and the amplitude threshold was set to 0.5 to identify most spike-like motion artifacts. After the artifacts were detected, the cubic spline interpolation was used for artifact correction, and then the spline interpolation function was subtracted from the original signals. Finally, to reconstruct the entire time series, signals were baseline corrected to ensure continuous time courses before and after motion artifact correction [34].

Based on the hemodynamic response function (HRF), the obtained HbO and HbR were block averaged within a time range from −2 to 35 s, and the baseline corrected using a reference epoch of −2 to 0 s. As the fNIRS channels were not in the exact location of EEG electrodes, a region of interest (ROI) was defined as the four fNIRS channels surrounding the corresponding EEG electrode, as shown in Fig. 1(b) using position C4 as an example. The average signal of these fNIRS channels represented the hemodynamic changes at the EEG channel location; thus, the EEG and hemodynamic signals can be considered acquired at approximately the same location. Since four subjects showed no significant HbO and HbR changes, only the data of the remaining sixteen subjects were used for further computation and analysis.

Considering that the movement-related HbO level is more evident than HbR, which is consistent with previous studies [35]. Therefore, the HbO is used in the subsequent analysis. We computed four commonly considered HbO features, i.e., the mean, difference, slope, and centroid values. The mean value was calculated from a 35-s period after movement onset (including the movement and rest period). It represented the total activation level of HbO. The difference value was computed as the mean value of the movement period (0-15 s), subtracting that of the rest period (15-35 s). It represented the

difference in HbO activation level before and after movement. During 2.5 and 7.5s, the HbO curve rose approximately linearly, and its slope differed between the two tasks (FES and VOL). Therefore, the HbO curve during 2.5-7.5 s was fitted using the least squares method to compute the slope value, which represented the HbO activation speed. The centroid value was the time when reaching half of the area enclosed by the HbO curve and the x-axis. The above HbO features were averaged over trials.

D. Neurovascular Coupling Evaluation

Transfer entropy (TE), as a benchmark method for detecting and quantifying information transfer between systems, was proposed by Schreiber in their work published in 2000 [36]. Its calculation does not need to assume any particular model of systems, i.e., model-free, and it can identify the directionality between interactions. The TE method has been proven to be applicable to a variety of neural signals, providing an effective method for the diagnosis, prevention, and treatment of diseases, as well as the evaluation of therapeutic effects [37], [38], [39], [40]. Here, we applied the TE method in NC evaluation to detect and quantify the interactions between the electrophysiological and hemodynamic variables. The TE value from time sequence$X = x_t$to$Y = y_t$is calculated as

$$TE_{x\to y} = \sum_{y_{t+u}, y_t^n, x_t^m} p\left(y_{t+u}, y_t^n, x_t^m\right) \log \frac{p\left(y_{t+u} \left| y_t^n, x_t^m\right.\right)}{P\left(y_{t+u} \left| y_t^n\right.\right)} \tag{2}$$

where $x_t^m = (x_t, \ldots, x_{t-m+1})$ and $y_t^n = (y_t, \ldots, y_{t-n+1})$. m and n denote the dimension of delay embedding vector of x_t and y_t, respectively. Additionally,$u$denotes the time lag, which reflects the effect of Y on X at different time scales. The TE values are between 0 and 1, and the larger the value, the more significant the information transfer is.

According to anatomy, EEG channels C4 and C4 located in the primary motor cortex that controls hand movements. The two channels have strong motion-related characteristics. Besides, FES can induce more ipsilateral cortical activation, which can also be observed by comparing these channels [41], [42]. Moreover, simple test and analysis processes can be easily integrated into clinical application systems. Some previous studies also chose the two channels for analysis [23], [43]. Therefore, the present study chose C3 and C4 channels for coupling analysis with hemodynamic signals at the same region. The EEG and fNIRS signals were further processed to find the underlying information interactions and correlations. The preprocessed EEG signals were decomposed into alpha (8-13 Hz) and beta (13-30 Hz) frequency bands. The EEG power envelope was computed as the absolute value of the Hilbert Transform and then smoothed. As the HbO change was generally more pronounced than the HbR, we calculated the HbO time courses of each ROI. The HbO signals of the four fNIRS channels around each EEG electrode were averaged to represent the HbO changes at the electrode position. TE was then calculated using the averaged HbO signal and the ERD curve of the EEG electrode. Finally, the EEG power envelope and the HbO signals were down-sampled to 2 Hz. Considering the instability of the first two tails, the data from the rest ten trials were used for analysis, resulting in a total length of 350 s (including the movement and rest periods). Both time series of EEG and HbO were aligned by markers and normalized between -1 and 1.

The TE between the above two time series was calculated in two directions, i.e., EEG to HbO ($TE_{\mathrm{EEG}\to\mathrm{HbO}}$) and HbO to EEG ($TE_{\mathrm{HbO}\to\mathrm{EEG}}$), with *MATLAB* using the *MuTE* toolbox developed by Montalto et al. [44]. Among several methods provided by the toolbox, we chose the *nnnue* method, which combines the non-uniform embedding and nearest neighbor estimator, for TE calculation considering its specificity and sensitivity to physiological time series.

E. Statistical Analysis

The Shapiro-Wilk test was performed to test the conformity of the HbO features and TE values to the normal distribution. The results showed that the data were significantly drawn from normally distributed populations at the 0.05 level. As four benchmark features (mean, difference, slope, and centroid) were computed to quantify HbO characteristics, the paired-sample t-test was used to assess the difference in HbO features between the two wrist extension tasks (VOL and FES). Statistical analyses were performed separately for electrode positions (C3 and C4) and features. Additionally, the TE values were computed to explore the coupling relationship between the EEG power envelope and HbO time courses. Therefore, another paired-sample t-test was used to assess the TE values between the two tasks. Statistical analyses were performed separately for positions, directions, and EEG frequency bands (alpha and beta), and the results were statistically different at $p < 0.05$.

III. Results and Analysis

A. Cerebral Hemodynamic Response

Fig. 2 shows the change of HbO and HbR concentration averaged over trials at the position C3 and C4 on the bilateral SMCs during the FES task. After the movement onset, the HbO concentration gradually increases and reaches the peak amplitude on the contralateral SMC. An initial increase is observed in HbR concentration, followed by a continuous decrease. The cerebral hemodynamic response lasts approximately 18 s after the movement offset. It is noted that the ipsilateral SMC shows a less pronounced hemodynamic response, but HbO reaches much higher amplitudes after movement cessation than during movement. The hemodynamic response process obtained from the VOL task is mostly similar, with slight differences as shown in Fig. 3. An initial decrease in HbO concentration is observed after the movement onset, followed by a rapid increase. The changing process of HbR is similar to that during the FES tasks. The hemodynamic response lasts for about 11 s after the movement offset. It is also more pronounced on the contralateral SMC.

Usually, a voluntary movement has a cerebral preparation stage before movement onset, which can be observed in the decrease in the spectral amplitude of central alpha/beta EEG rhythms [45]. Brain activation requires oxygen consumption, which decreases HbO and increases HbR concentration immediately at the movement onset. To deliver more energy to this brain area, functional hyperemia causes higher CBF while HbO concentration begins to increase and reaches its peak. At the same time, the HbR is washed out and its

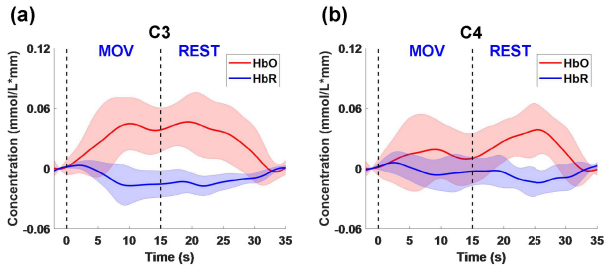

Fig. 2. Concentration changes of HbO and HbR at the position C3 and C4, averaged over subjects in the FES tasks.

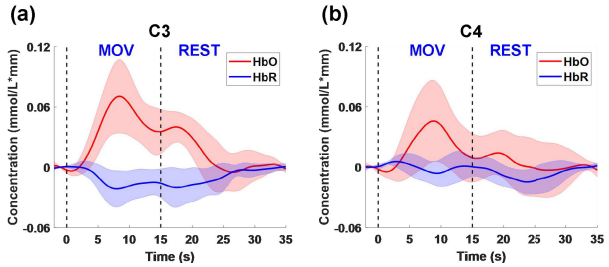

Fig. 3. Concentration changes of HbO and HbR at the position C3 and C4, averaged over subjects in the VOL tasks.

concentration decreases. In contrast, a FES-induced movement has no movement preparation stage [46], and thus there is no requirement for oxygen pre-consumption as voluntary movements. Therefore, the initial decrease in HbO concentrations in the FES tasks is not obvious. Besides, slower HbO activation and longer lasting hemodynamic response can be found in the FES tasks compared with the VOL tasks.

Fig. 4 compares the four HbO features (mean, difference, slope, and centroid) at the position C3 and C4 for the two tasks. As shown in Fig. 4(a) and (b), no significant difference is found in the HbO mean between the two tasks, meaning a similar activation level by both tasks. As shown in Fig. 4(c) and (d), the HbO difference is significantly smaller in the FES task at both the position C3 and C4. Therefore, the activation level after movement is higher in the FES tasks. Fig. 4(e) and (f) shows that HbO slope in the VOL task is more significant than that in the FES task. This indicates that the VOL movements may feature a more rapid HbO activation speed. Fig. 4(g) and (h) shows that the HbO centroid is significantly higher in the FES task, showing that the FES-induced movements may feature a more prolonged activation.

B. Event-Related Spectral Perturbation

Fig. 5(a) and Fig. 6(a) show the time-frequency maps of ERD/ERS during a FES task for the position C3 and C4, respectively. The results were averaged over subjects. The blue color on the time-frequency map indicates a decrease in power (ERD), while the orange color indicates an increase in power (ERS). The ERD/ERS time-frequency maps clearly show that a pronounced ERD occurs in EEG alpha and beta bands on bilateral SMCs during a 15-s movement period, and ERS bursts after the movement cessation.

Fig. 5(b) and Fig. 6(b) show the ERD/ERS time courses during the FES task for C3 and C4, respectively. During the movement period, the alpha EEG power decreases to a minimum value and begins to rebound. However, the beta EEG power can maintain a steady value and finally begin to increase. After the movement offset, EEG power in the alpha and beta bands increases rapidly to a maximum value, generally noted as the post-movement ERS, and finally decreases to the baseline.

The ERD/ERS time-frequency maps and time courses on bilateral SMCs in the VOL task are similar to those in the

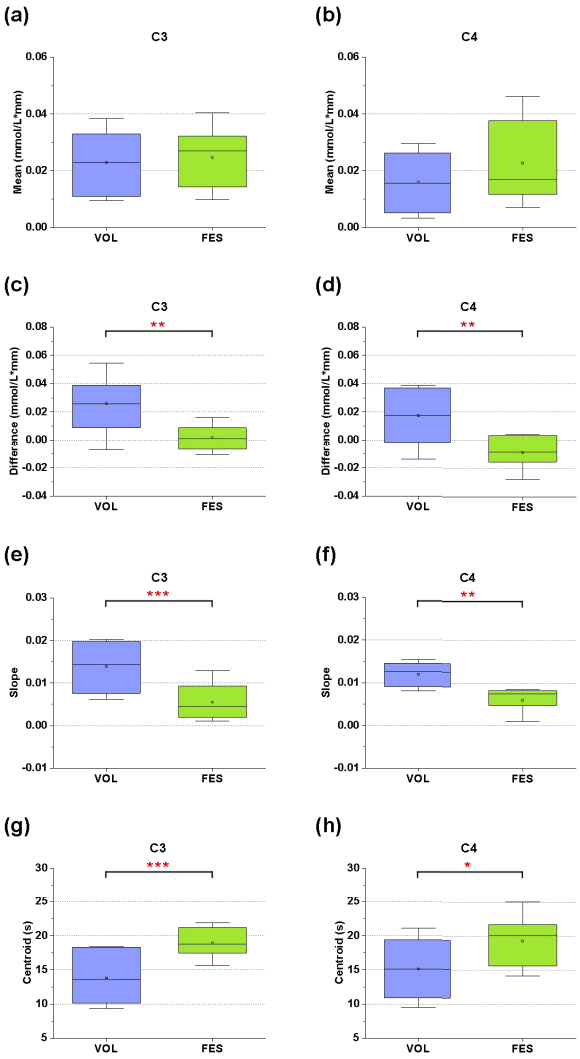

Fig. 4. Comparison of HbO features at the position C3 and C4 in two tasks, where (a) and (b) correspond to the HbO mean during a 35 s-period including movement and rest, (c) and (d) correspond to the HbO difference between 15-s movement and 20-s rest period, (e) and (f) correspond to HbO slope between 2.5 and 7.5 s, and (g) and (h) correspond to HbO centroid in the same duration as (a) and (b). *: p<0.05, **: p<0.01,***: p<0.001.

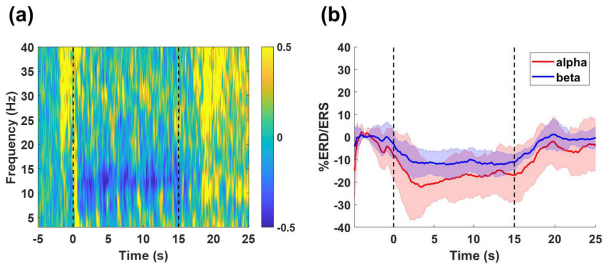

Fig. 5. (a) Averaged time-frequency map and (b) time courses of ERD/ERS at the position C3 in the FES task. The blue color in (a) indicates a decrease in power (ERD), while the orange color indicates an increase in power (ERS).

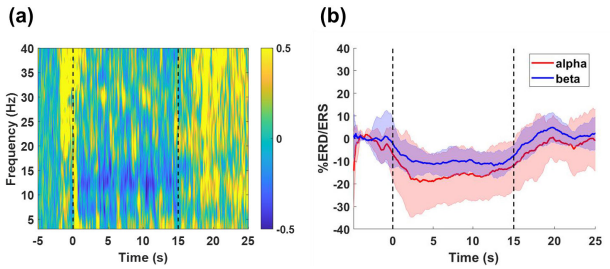

Fig. 6. (a) Averaged time-frequency map and (b) time courses of ERD/ERS at the position C4 in the FES task. The blue color in (a) indicates a decrease in power (ERD), while the orange color indicates an increase in power (ERS).

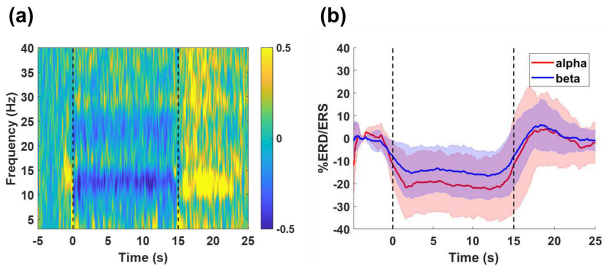

Fig. 7. (a) Averaged time-frequency map and (b) time courses of ERD/ERS at the position C3 in the VOL task. The blue color in (a) indicates a decrease in power (ERD), while the orange color indicates an increase in power (ERS).

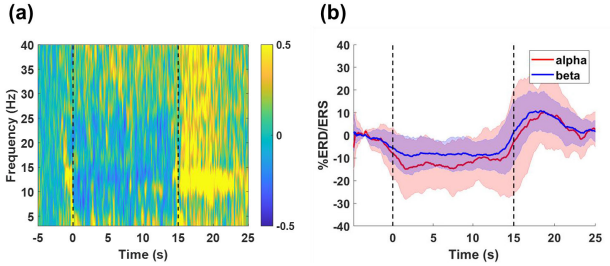

Fig. 8. (a) Averaged time-frequency map and (b) time courses of ERD/ERS at the position C4 in the VOL task. The blue color in (a) indicates a decrease in power (ERD), while the orange color indicates an increase in power (ERS).

FES task, as shown in Figs. 7 and 8. However, a more considerable power decrease in the alpha and beta bands during the movement period is observed in the VOL task. Besides, the alpha EEG power decreases to a platform value, corresponding to those described in the literature [47], [48], instead of the rebounding trend observed during the FES task.

C. NC Evaluation

We calculated the TE values between the alpha/beta power envelope and HbO time courses at the same electrode position to explore the NC relationship between the electrophysiological and hemodynamic variables. Fig. 9 shows the processed EEG beta power envelope and HbO time courses for TE calculation from a typical subject in the FES task. Periodic but inverse changes can be observed from the two variables during movement periods.

As shown in Figs. 10 and 11, a bidirectional information interaction can be found between the two variables, and the coupling strength varies in different directions. We used $TE_{\mathrm{EEG}\rightarrow\mathrm{HbO}}$ to denote the TE from EEG to HbO, and $TE_{\mathrm{HbO}\rightarrow\mathrm{EEG}}$ to denote TE from HbO to EEG. According to

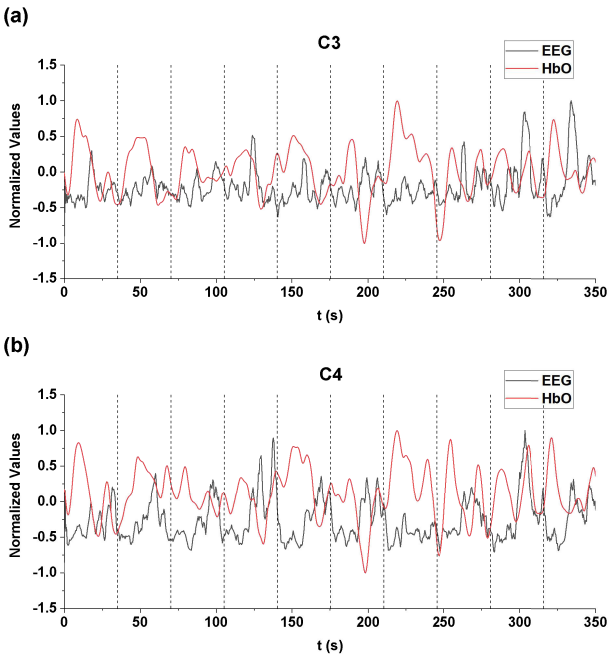

Fig. 9. EEG beta power envelope and HbO time courses for a typical subject in a FES task. The 350 s-period was divided into ten trials by vertical dash lines.

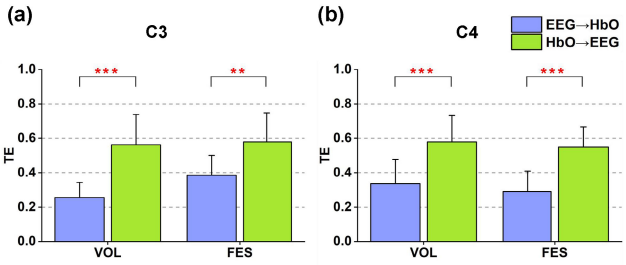

Fig. 10. Comparison of TE values between the EEG alpha band and HbO time series at the position C3 and C4 for the two tasks. TE values were normalized between 0 and 1 for better visualization. *: p<0.05, **: p<0.01, ***: p<0.001.

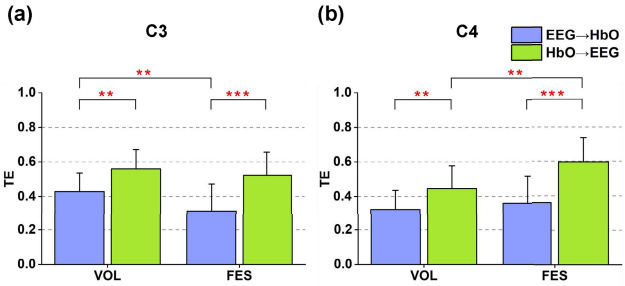

Fig. 11. Comparison of TE values between the EEG beta band and HbO time series at the position C3 and C4 for the two tasks. TE values were normalized between 0 and 1 for better visualization. ∗: p<0.05, **: p<0.01, ***: p<0.001.

the calculation, the $TE_{\mathrm{HbO}\rightarrow\mathrm{EEG}}$ is found to be significantly higher than the $TE_{\mathrm{EEG}\rightarrow\mathrm{HbO}}$ on bilateral SMCs in both tasks. Hemodynamic signals directly reflect metabolic demand, and blood and oxygen supply are essential by providing energy and supporting brain neural activities. This result was also consistent with a previous related study [49].

Especially, Fig. 10 compares the TE values calculated using the alpha EEG power envelope and HbO time series at the position C3 and C4 for the two tasks, where no significant

difference is found. Fig. 11 compares TE values calculated using the beta EEG power envelope and HbO time series at the position C3 and C4 for the two tasks, where significant differences are achieved. At the contralateral C3, the paired-sample t-test results show that the $TE_{\mathrm{EEG}\rightarrow\mathrm{HbO}}$ is more significant in the VOL task (p<0.05). The underlying reason might be that a voluntary wrist extension is a spontaneous human movement, during which the EEG activates before movement onset, and the cortex activation induces hemodynamic changes. However, a FES task is an activation caused by passive input, and therefore its effect cannot be equated entirely with that of a voluntary movement. At the ipsilateral C4, the $TE_{\mathrm{HbO}\rightarrow\mathrm{EEG}}$ is more significant in the FES task (p<0.01), which indicates that the ipsilateral $TE_{\mathrm{HbO}\rightarrow\mathrm{EEG}}$ is enhanced by FES. This phenomenon is in accordance with some previous literature, which have also shown that FES can enhance the ipsilateral brain activation [42], [48]. Therefore, it is proved that FES can potentially improve the regulatory effect of ipsilateral cerebral blood flow on neuronal activities, hence providing a substantial piece of evidence for FES therapy.

IV. Discussion

A. Brain Rhythmic Activities and Cerebral Hemodynamic Responses

In this work, the brain rhythmic activities observed on the contralateral SMC during the VOL tasks are consistent with some previous study [21]. However, the results on the ipsilateral SMC differ from theirs, which showed that the ERD/ERS on ipsilateral SMC was much less noticeable than the contralateral one. The possible reason might be that different movement paradigms were executed, i.e., self-paced finger movements were performed in that study, while repetitive maximum wrist movements were investigated in this work. Our results show significant bilateral ERD/ERS, the same as a previously reported study that involved continuous, repetitive, and long-duration hand movements [50].

In the FES tasks, similar ERD/ERS phenomena and HbO/HbR responses were observed. The results of HbO features indicate that a similar HbO activation level (measured by HbO mean from 0 to 35 s) on bilateral SMCs can be achieved by FES compared to the VOL tasks. Moreover, a higher and longer-lasting HbO activation was observed after the movement offset in FES tasks, revealed by the HbO difference and centroid, even though the HbO activation speed was slower. However, the results achieved by us differ from the HbO feature comparison between the FES and VOL movements reported in [35]. That study showed that mean cortical regional changes of HbO concentration on the contralateral SMC were significantly smaller in the FES-induced knee extensions than the VOL movements, because FES cannot induce a movement range equal to a voluntary task there. In our experiments, the maximum wrist extension was performed to ensure the same contraction level in both the VOL and FES tasks.

Besides, in this work we did not find a pre-movement ERD before the movement onset in VOL tasks because the markers displayed on the computer screen were used to remind subjects to move their wrists, which was not the exact movement start time. The same situation existed in the FES tasks, where the markers were used to remind the experimenter to start FES. Therefore, the ERD occurred a little bit later than the movement onset. Since some previous studies have compared the pre-movement ERD patterns of FES and VOL movements [21], [46] and thus our study did not focus on this issue.

Nevertheless, the present results have demonstrated that FES can induce similar changes in amplitudes (ERD/ERS) of EEG rhythms and cerebral hemodynamic responses (HbO and HbR) on bilateral SMCs as the VOL movements. As commonly known, a VOL movement is self-initiated, while FES is a passive activation process caused by external input. However, FES could effectively promote the activation of related cortical areas and improve CBF perfusion.

B. NC Evaluation

As there exists no ideal temporal and spatial correspondence between the local neural activities and cerebral hemodynamic response, to quantify the underlying NC relationship is relatively challenging. Although some EEG-fNIRS combined studies have been conducted for NC analysis based on different tasks, however, only few focused on quantitative evaluation. As reported, Pearson Correlation Coefficient (cc) is a common index used to analyze NC relationship by comparing different tasks, where a negative cc was found between HbO and alpha/beta EEG rhythms, and a positive cc was found between HbR and the above rhythms during motor executions [21], [22]. However, cc can only measure a linear correlation but cannot describe the nonlinear coupling characteristics in EEG and hemodynamic signals.

In the present study, we used TE to explore and quantify the interaction between EEG and hemodynamic signals. It shows a strong capability in detecting the directional causal relationship of biomedical time series with nonlinear characteristics [51], [52]. Specifically, we calculated TE between the EEG power envelope and HbO time course, demonstrating a bidirectional interaction in between. The result shows that $TE_{\mathrm{HbO}\rightarrow\mathrm{EEG}}$ is considerably larger than $TE_{\mathrm{EEG}\rightarrow\mathrm{HbO}}$. Previous studies showed hemodynamic responses are slower than neuronal activities in several seconds [21]; however, the above TE results obtained do not contradict the slow response and low temporal resolution of HbO signals. Higher $TE_{\mathrm{HbO}\rightarrow\mathrm{EEG}}$ means that HbO has a predominant driving influence on EEG. The results indicate that HbO is the source of energy consumption. Long-duration neural activities rely on a continuous energy supply through the CBF, which corresponds to the mechanism of NC.

The central beta EEG rhythms can demonstrate a high task and movement specificity. Beta rhythms are desynchronized before and during voluntary movements. Pre-movement beta-ERD has been related to movement planning and preparation, and post-movement beta ERS reflects the deactivated motor cortex [46], [47]. In the experiment we found significant differences in TE values calculated using the beta EEG rhythms and HbO between the two tasks, where on the contralateral SMC, $TE_{\mathrm{EEG}\rightarrow\mathrm{HbO}}$ in the FES tasks is significantly smaller than that in the VOL tasks. Since $TE_{\mathrm{EEG}\rightarrow\mathrm{HbO}}$ reflects the regulatory effect of beta activation on hemodynamics, and thus it can say the beta activation has a stronger regulatory effect on hemodynamics during voluntary movements. On the ipsilateral SMC, however, $TE_{\mathrm{HbO}\rightarrow\mathrm{EEG}}$ in the FES tasks is significantly larger than that in the VOL tasks. Since $TE_{\mathrm{HbO}\rightarrow\mathrm{EEG}}$ indicates the beta activation relying on the continuous energy supply

though CBF, so the CBF perfusion is improved on the ipsilateral SMC by the FES-induced movements, resulting in an enhanced regulatory effect on beta rhythms.

The above TE results may provide evidence from a perspective of information transfer, where a different activation mechanism exists between the two tasks. In addition, the NC relationship can be quantified though the TE analysis, which is proved to be a useful objective biomarker of brain activation.

C. Study Significance

The present study can be considered as a necessary first step for the investigation into the neural rehabilitation mechanism of FES. The brain injuries are complex and different among stroke patients, and the results obtained from healthy subjects may provide a control condition and demonstrate the feasibility of proposed method.

The neurovascular coupling mechanisms obtained in the present study can provide the following information and suggestions for FES-based neurorehabilitation. In the early stages of after-stroke rehabilitation (acute and subacute stages), patients are unable to perform voluntary training due to paralysis. Therefore, FES can be suggested as a primary therapy to activate the peripheral-central nerve pathway, induce the neurovascular coupling response, produce stable and lasting HbO activation, and thus improve the perfusion of the affected side of the brain cortex [53]. During the critical window period of neurological function recovery (3-6 months after stroke), it is recommended to use voluntary training assisted with FES to promote the neurorehabilitation process, since voluntary movements can significantly increase the hemodynamic response speed of the bilateral primary motor cortex [54]. We also recommend regularly using multimodal EEG-fNIRS synchronous monitoring to assess the patient's neurovascular decoupling based on TE and tracking TE changes to evaluate NC reconstruction and rehabilitation progress [55]. In conclusion, the results can provide specific evidence-based support for clinical FES therapy.

D. Study Limitations and Future Directions

This study has several limitations. We acquired data from several female subjects in preliminary experiments; however, the fNIRS signals were weak and noisy due to their long and thick hair. Therefore, we just recruited male subjects in the present study and ignored the possible gender influence. Referring to previous literature that study brain activation or analyze NC based on simultaneous EEG-fNIRS [21], [23], [35], [56], [57], [58], the present study recruited 20 participants and finally used data of 16 subjects for analysis because HbO and HbR of 4 subjects didn't show apparent changes. Like most movement-related fNIRS studies [35], [58], the HbO changes were more senstive than HbR in the present study; therefore, we just computed the HbO feature and TE between the HbO and ERD curves. In addition, HbT, the sum of HbO and HbR, is another critical fNIRS parameter representing total blood volume changes.

In future work, we will recruit more participants, covering different genders and ages. We will also expand the calculation and analysis to more channels and parameters (including HbR and HbT) to obtain the NC law in more cortical regions and explore more biomarkers.

V. Conclusion

In the present study, the brain rhythmic activities and cerebral hemodynamic responses during FES-induced wrist movements were investigated and compared with voluntary movements by analyzing the coupling behaviors of simultaneously recorded EEG-fNIRS signals. The results indicated that FES could induce similar ERD/ERS patterns but with higher and longer-lasting HbO changes after the cessation of movements. TE calculation results showed a bidirectional information transfer relationship between EEG and HbO time courses but with different intensities. This work may prove TE as an objective biomarker for quantifying brain activation, and provide evidence of a different activation mechanism between the FES-induced and voluntary movements.

References

[1] E. Ambrosini, M. Parati, G. Ferriero, A. Pedrocchi, and S. Ferrante, "Does cycling induced by functional electrical stimulation enhance motor recovery in the subacute phase after stroke? A systematic review and meta-analysis," *Clin. Rehabil.*, vol. 34, no. 11, pp. 1341–1354, Nov. 2020.

[2] N. Kapadia, B. Moineau, and M. R. Popovic, "Functional electrical stimulation therapy for retraining reaching and grasping after spinal cord injury and stroke," *Frontiers Neurosci.*, vol. 14, Jul. 2020, Art. no. 00718.

[3] C. Marquez-Chin and M. R. Popovic, "Functional electrical stimulation therapy for restoration of motor function after spinal cord injury and stroke: A review," *Biomed. Eng. OnLine*, vol. 19, no. 1, Dec. 2020, Art. no. 34.

[4] S. Luo, H. Xu, Y. Y. Zuo, X. Liu, and A. H. All, "A review of functional electrical stimulation treatment in spinal cord injury," *Neuromol. Med.*, vol. 22, no. 4, pp. 447–463, Jan. 2020.

[5] A. Jannati, L. M. Oberman, A. Rotenberg, and A. Pascual-Leone, "Assessing the mechanisms of brain plasticity by transcranial magnetic stimulation," *Neuropsychopharmacology*, vol. 48, no. 1, pp. 191–208, Jan. 2023.

[6] W. Young, "Electrical stimulation and motor recovery," *Cell Transplantation*, vol. 24, no. 3, pp. 429–446, Mar. 2015.

[7] P. S. Katz, "Evolution of central pattern generators and rhythmic behaviours," *Phil. Trans. Roy. Soc. B, Biol. Sci.*, vol. 371, no. 1685, Jan. 2016, Art. no. 20150057.

[8] W. M. Zhu, A. Neuhaus, D. J. Beard, B. A. Sutherland, and G. C. DeLuca, "Neurovascular coupling mechanisms in health and neurovascular uncoupling in Alzheimer's disease," *Brain*, vol. 145, no. 7, pp. 2276–2292, Jul. 2022.

[9] A. S. Salinet et al., "Impaired cerebral autoregulation and neurovascular coupling in middle cerebral artery stroke: Influence of severity?" *J. Cerebral Blood Flow Metabolism*, vol. 39, no. 11, pp. 2277–2285, Nov. 2019.

[10] J. A. H. R. Claassen, D. H. J. Thijssen, R. B. Panerai, and F. M. Faraci, "Regulation of cerebral blood flow in humans: Physiology and clinical implications of autoregulation," *Physiolog. Rev.*, vol. 101, no. 4, pp. 1487–1559, Oct. 2021.

[11] C. Iadecola, "The neurovascular unit coming of age: A journey through neurovascular coupling in health and disease," *Neuron*, vol. 96, no. 1, pp. 17–42, Sep. 2017.

[12] H. Girouard and C. Iadecola, "Neurovascular coupling in the normal brain and in hypertension, stroke, and Alzheimer disease," *J. Appl. Physiol.*, vol. 100, no. 1, pp. 328–335, Jan. 2006.

[13] M. K. Yeung and V. W. Chu, "Viewing neurovascular coupling through the lens of combined EEG–fNIRS: A systematic review of current methods," *Psychophysiology*, vol. 59, no. 6, Jun. 2022, Art. no. 14054.

[14] A. M. Chiarelli, F. Zappasodi, F. Di Pompeo, and A. Merla, "Simultaneous functional near-infrared spectroscopy and electroencephalography for monitoring of human brain activity and oxygenation: A review," *Neurophotonics*, vol. 4, no. 4, Aug. 2017, Art. no. 041411.

[15] M. X. Cohen, "Where does EEG come from and what does it mean?" *Trends Neurosci.*, vol. 40, no. 4, pp. 208–218, Apr. 2017.

[16] P. L. Nunez, M. D. Nunez, and R. Srinivasan, "Multi-scale neural sources of EEG: Genuine, equivalent, and Representative. A tutorial review," *Brain Topography*, vol. 32, no. 2, pp. 193–214, Mar. 2019.

[17] P. Pinti et al., "The present and future use of functional near-infrared spectroscopy (fNIRS) for cognitive neuroscience," *Ann. N.Y. Acad. Sci.*, vol. 1464, no. 1, pp. 5–29, Aug. 2018.

[18] J. S. Burma et al., "Quantifying neurovascular coupling through a concurrent assessment of arterial, capillary, and neuronal activation in humans: A multimodal EEG-fNIRS-TCD investigation," *NeuroImage*, vol. 302, Nov. 2024, Art. no. 120910.

[19] R. B. Buxton, K. Uludağ, D. J. Dubowitz, and T. T. Liu, "Modeling the hemodynamic response to brain activation," *NeuroImage*, vol. 23, pp. S220–S233, 2004.

[20] L. Li, M. Zhang, Y. Chen, K. Wang, G. Zhou, and Q. Huang, "TAGL: Temporal-guided adaptive graph learning network for coordinated movement classification," *IEEE Trans. Ind. Informat.*, vol. 20, no. 11, pp. 12554–12564, Nov. 2024.

[21] P. Lachert, D. Janusek, P. Pulawski, A. Liebert, D. Milej, and K. J. Blinowska, "Coupling of oxy- and deoxyhemoglobin concentrations with EEG rhythms during motor task," *Sci. Rep.*, vol. 7, no. 1, Nov. 2017, Art. no. 15414.

[22] M. S. Al-Quraishi, I. Elamvazuthi, T. B. Tang, M. Al-Qurishi, S. H. Adil, and M. Ebrahim, "Bimodal data fusion of simultaneous measurements of EEG and fNIRS during lower limb movements," *Brain Sci.*, vol. 11, no. 6, p. 713, May 2021.

[23] Z. Wang et al., "BCI monitor enhances electroencephalographic and cerebral hemodynamic activations during motor training," *IEEE Trans. Neural Syst. Rehabil. Eng.*, vol. 27, no. 4, pp. 780–787, Apr. 2019.

[24] A. von Lühmann, J. Addesa, S. Chandra, A. Das, M. Hayashibe, and A. Dutta, "Neural interfacing non-invasive brain stimulation with NIRS-EEG joint imaging for closed-loop control of neuroenergetics in ischemic stroke," in *Proc. 8th Int. IEEE/EMBS Conf. Neural Eng. (NER)*, Shanghai, China, May 2017, pp. 349–353.

[25] A. Dutta, A. Jacob, S. R. Chowdhury, A. Das, and M. A. Nitsche, "EEG-NIRS based assessment of neurovascular coupling during anodal transcranial direct current stimulation—A stroke case series," *J. Med. Syst.*, vol. 39, no. 4, pp. 1–9, Apr. 2015.

[26] D. Perpetuini et al., "Working memory decline in Alzheimer's disease is detected by complexity analysis of multimodal EEG-fNIRS," *Entropy*, vol. 22, no. 12, p. 1380, Dec. 2020.

[27] A. M. Chiarelli et al., "Evidence of neurovascular un-coupling in mild Alzheimer's disease through multimodal EEG-fNIRS and multivariate analysis of resting-state data," *Biomedicines*, vol. 9, no. 4, p. 337, Mar. 2021.

[28] A. Delorme and S. Makeig, "EEGLAB: An open source toolbox for analysis of single-trial EEG dynamics including independent component analysis," *J. Neurosci. Methods*, vol. 134, no. 1, pp. 9–21, Mar. 2004.

[29] K. Nakayashiki, M. Saeki, Y. Takata, Y. Hayashi, and T. Kondo, "Modulation of event-related desynchronization during kinematic and kinetic hand movements," *J. NeuroEng. Rehabil.*, vol. 11, no. 1, pp. 1–9, Dec. 2014.

[30] G. Pfurtscheller and F. H. Lopes da Silva, "Event-related EEG/MEG synchronization and desynchronization: Basic principles," *Clin. Neurophysiol.*, vol. 110, no. 11, pp. 1842–1857, Nov. 1999.

[31] Q. Li et al., "Effects of the multisensory rehabilitation product for home-based hand training after stroke on cortical activation by using NIRS methods," *Neurosci. Lett.*, vol. 717, Jan. 2020, Art. no. 134682.

[32] R. Di Lorenzo et al., "Recommendations for motion correction of infant fNIRS data applicable to multiple data sets and acquisition systems," *NeuroImage*, vol. 200, pp. 511–527, Oct. 2019.

[33] X. Hu, C. Zhuang, F. Wang, Y.-J. Liu, C.-H. Im, and D. Zhang, "fNIRS evidence for recognizably different positive emotions," *Frontiers Hum. Neurosci.*, vol. 13, Apr. 2019, Art. no. 120.

[34] M. A. Yücel et al., "Best practices for fNIRS publications," *Neurophotonics*, vol. 8, no. 1, Jan. 2021, Art. no. 012101.

[35] T.-Y. Lin, J.-S. Wu, L. L. Lin, T.-C. Ho, P.-Y. Lin, and J. J. Chen, "Assessments of muscle oxygenation and cortical activity using functional near-infrared spectroscopy in healthy adults during hybrid activation," *IEEE Trans. Neural Syst. Rehabil. Eng.*, vol. 24, no. 1, pp. 1–9, Jan. 2016.

[36] T. Schreiber, "Measuring information transfer," *Phys. Rev. Lett.*, vol. 85, no. 2, pp. 461–464, Jul. 2000.

[37] T. Wang, J. Yang, Y. Song, F. Pang, X. Guo, and Y. Luo, "Interactions of central and autonomic nervous systems in patients with sleep apnea–hypopnea syndrome during sleep," *Sleep Breath.*, vol. 26, no. 2, pp. 621–631, Jul. 2021.

[38] C. Ciprian, K. Masychev, M. Ravan, A. Manimaran, and A. Deshmukh, "Diagnosing schizophrenia using effective connectivity of resting-state EEG data," *Algorithms*, vol. 14, no. 5, p. 139, Apr. 2021.

[39] D. McKenna and J. Peever, "Degeneration of rapid eye movement sleep circuitry underlies rapid eye movement sleep behavior disorder," *Movement Disorders*, vol. 32, no. 5, pp. 636–644, May 2017.

[40] X. Wang, W. Li, R. Song, D. Ao, H. Hu, and L. Li, "Corticomuscular coupling alterations during elbow isometric contraction correlated with clinical scores: An fNIRS-sEMG study in stroke survivors," *IEEE Trans. Neural Syst. Rehabil. Eng.*, vol. 33, pp. 696–704, 2025.

[41] M. Hervault, P.-G. Zanone, J.-C. Buisson, and R. Huys, "Cortical sensorimotor activity in the execution and suppression of discrete and rhythmic movements," *Sci. Rep.*, vol. 11, no. 1, Nov. 2021, Art. no. 22364.

[42] S. Qiu et al., "Event-related beta EEG changes during active, passive movement and functional electrical stimulation of the lower limb," *IEEE Trans. Neural Syst. Rehabil. Eng.*, vol. 24, no. 2, pp. 283–290, Feb. 2016.

[43] X. Shi, H. Wang, B. Li, Y. Qin, C. Peng, and Y. Lu, "Fusion analysis of EEG-fNIRS multimodal brain signals: A multitask classification algorithm incorporating spatial–temporal convolution and dual attention mechanisms," *IEEE Trans. Instrum. Meas.*, vol. 74, pp. 1–12, 2025.

[44] A. Montalto, L. Faes, and D. Marinazzo, "MuTE: A MATLAB toolbox to compare established and novel estimators of the multivariate transfer entropy," *PLoS ONE*, vol. 9, no. 10, Oct. 2014, Art. no. e109462.

[45] E. Houdayer, S.-J. Lee, and M. Hallett, "Cerebral preparation of spontaneous movements: An EEG study," *Clin. Neurophysiol.*, vol. 131, no. 11, pp. 2561–2565, Nov. 2020.

[46] G. R. Müller, C. Neuper, R. Rupp, C. Keinrath, H. J. Gerner, and G. Pfurtscheller, "Event-related beta EEG changes during wrist movements induced by functional electrical stimulation of forearm muscles in man," *Neurosci. Lett.*, vol. 340, no. 2, pp. 143–147, Apr. 2003.

[47] G. Tacchino, M. Gandolla, S. Coelli, R. Barbieri, A. Pedrocchi, and A. M. Bianchi, "EEG analysis during active and assisted repetitive movements: Evidence for differences in neural engagement," *IEEE Trans. Neural Syst. Rehabil. Eng.*, vol. 25, no. 6, pp. 761–771, Jun. 2017.

[48] W. Cho, C. Vidaurre, J. An, N. Birbaumer, and A. Ramos-Murguialday, "Cortical processing during robot and functional electrical stimulation," *Frontiers Syst. Neurosci.*, vol. 17, Mar. 2023, Art. no. 1045396.

[49] R. Khanal, "Brain connectivity during different sleep stages using EEG and NIRS," M. S. thesis, Dept. College Sci. Eng., Flinders Univ., Adelaide, SA, Australia, 2019.

[50] N. Erbil and P. Ungan, "Changes in the alpha and beta amplitudes of the central EEG during the onset, continuation, and offset of long-duration repetitive hand movements," *Brain Res.*, vol. 1169, pp. 44–56, Sep. 2007.

[51] J. Liu, G. Tan, Y. Sheng, and H. Liu, "Multiscale transfer spectral entropy for quantifying corticomuscular interaction," *IEEE J. Biomed. Health Informat.*, vol. 25, no. 6, pp. 2281–2292, Jun. 2021.

[52] J. Morales et al., "Model-based evaluation of methods for respiratory sinus arrhythmia estimation," *IEEE Trans. Biomed. Eng.*, vol. 68, no. 6, pp. 1882–1893, Jun. 2021.

[53] H.-C. Pan et al., "Neurovascular function recovery after focal ischemic stroke by enhancing cerebral collateral circulation via peripheral stimulation-mediated interarterial anastomosis," *Neurophotonics*, vol. 4, no. 3, Sep. 2017, Art. no. 035003.

[54] R. Borzuola, F. Quinzi, M. Scalia, S. Pitzalis, F. Di Russo, and A. Macaluso, "Acute effects of neuromuscular electrical stimulation on cortical dynamics and reflex activation," *J. Neurophysiol.*, vol. 129, no. 6, pp. 1310–1321, Jun. 2023.

[55] X. Sun et al., "Current implications of EEG and fNIRS as functional neuroimaging techniques for motor recovery after stroke," *Med. Rev.*, vol. 4, no. 6, pp. 492–509, Dec. 2024.

[56] P. Pinti, M. F. Siddiqui, A. D. Levy, E. J. H. Jones, and I. Tachtsidis, "An analysis framework for the integration of broadband NIRS and EEG to assess neurovascular and neurometabolic coupling," *Sci. Rep.*, vol. 11, no. 1, Feb. 2021, Art. no. 3977.

[57] R. Li, C. Zhao, C. Wang, J. Wang, and Y. Zhang, "Enhancing fNIRS analysis using EEG rhythmic signatures: An EEG-informed fNIRS analysis study," *IEEE Trans. Biomed. Eng.*, vol. 67, no. 10, pp. 2789–2797, Oct. 2020.

[58] J. Lin, J. Lu, Z. Shu, J. Han, and N. Yu, "Subject-specific modeling of EEG-fNIRS neurovascular coupling by task-related tensor decomposition," *IEEE Trans. Neural Syst. Rehabil. Eng.*, vol. 32, pp. 452–461, 2024.